

Self-organized growth of Ni nanoparticles on a cobalt-oxide thin film induced by a buried misfit dislocation network

P. Torelli,¹ E. A. Soares,² G. Renaud,³ L. Gragnaniello,^{1,4} S. Valeri,^{1,4} X. X. Guo,³ and P. Luches¹

¹*INFN-CNR, National Research Centre for nanoStructures and bioSystems at Surfaces (S3), Via Campi 213/A, 41100 Modena, Italy*

²*Departamento de Física, Universidade Federal de Minas Gerais, C.P. 702, 30123-970 Belo Horizonte, MG, Brazil*

³*CEA-Grenoble, Département de Recherche Fondamentale sur la Matière Condensée/SP2M/NRS,*

17 rue de Martyrs, 38054, Grenoble, France

⁴*Dipartimento di Fisica, Università di Modena e Reggio Emilia, Via Campi 213/A, 41100 Modena, Italy*

(Received 10 December 2007; published 25 February 2008)

We report on a clear tendency toward organized growth, at room temperature, of Ni nanoislands deposited on a CoO(001) nanopatterned surface. The 9.2 nm square surface patterning consists in a periodic displacement field induced at the surface by an underlying interfacial dislocations network that is buried at the interface between the 5 nm thick CoO(001) thin film and the Ag(001) substrate. Grazing incidence small and wide angle x-ray scattering (GISAXS and GIXD) performed *in situ*, during growth, reveal that the nucleation of Ni particles is driven by the underlying dislocation distribution. The tendency for organization is confirmed by scanning tunneling microscopy (STM), which also reveals a quite narrow size distribution of the Ni nanoparticles around 5 nm width and 0.6 nm height.

DOI: [10.1103/PhysRevB.77.081409](https://doi.org/10.1103/PhysRevB.77.081409)

PACS number(s): 81.16.Dn, 61.72.Hh, 68.35.-p

Ordered assemblies of monodisperse nanoparticles on surfaces are of a great interest for fundamental and technological research, especially in the case of metallic nanoparticles on oxide substrates, in view of their applications in nanomagnetism¹ and catalysis.² The production of these systems is now possible thanks to a variety of techniques such as lithography or ion beam sculpting, but these techniques are expensive and require long preparation procedures. The self-organized growth of atoms in the first stage of an overlayer growth is seen as a smart solution to overcome the drawbacks of the so-called top-down techniques. To become a reliable alternative, the self-assembling process has to demonstrate the capability of giving rise to collections of nanoparticles with a narrow size distribution and an ordered spatial arrangement. The major problem in order to achieve this goal is represented by the random deposition and diffusion of atoms on surfaces. This process has been successfully controlled by deposition on surfaces displaying a regular network of preferential nucleation and growth sites. It has been demonstrated for surfaces having particular reconstructions³⁻⁵ or on few monolayers thin films presenting a coincidence site lattice with the substrate.^{6,7} These experiments have demonstrated the potential of the self-organized growth process, producing well-ordered collections of nanoparticles of a given size and shape. Nevertheless, until now, the few substrates used as templates for self-organized growth are either metallic or semiconductor surfaces, and the periodicities (a few nanometers) and deposits (much less than 0.1 nm) were extremely small. In addition, in the great majority of cases, the substrates are almost bidimensional. It has been suggested⁸ that the strain field created by buried interfacial dislocations can propagate into a film of several nanometer of thickness resulting in a surface with a nanostructuration suitable for the successive growth of ordered self-assembled nanoparticles. However, this was achieved only in very few systems,⁹⁻¹¹ and never on oxide films. Another limitation to the application of the self-

ordering process is represented by the deposition temperature; in many works the spatial order is obtained at low temperatures because the thermal energy at room temperature is sufficient to overcome the energy barrier between different nucleation sites. Hence, obtaining a self-organized growth of metallic nanoparticles on the surface of thick-enough thin films, at room temperature and over a larger periodicity of the order of 10 nm remains a challenge.

In this work, we show that it is possible to obtain an ordered collection of metallic clusters of ~ 5 nm lateral size and 0.6 nm height on an oxide film of 5 nm of thickness, at room temperature, and on a network of 10 nm period. Due to the 3.25% lattice mismatch between the CoO overlayer and the Ag(001) substrate, a square network of dislocations forms at the CoO/Ag(001) interface. The interfacial dislocation network creates a periodic atomic displacement field that extends up to the surface, thus influencing the growth of a Ni overlayer, which develops a spatially ordered distribution of clusters.

Grazing incidence x-ray diffraction (GIXD) and small angle x-ray scattering (GISAXS) experiments were performed at the BM 32 beamline of the European Synchrotron Radiation Facility (Grenoble, France),^{12,13} and scanning tunneling microscopy (STM) measurements were carried out at the Sesamo laboratory of the S3 National Research Centre (Modena, Italy). Both experimental setups are UHV systems (base pressure below 1×10^{-10} mbar) optimized for the preparation of surfaces and thin films. The x-ray measurements were performed with an energy of 18 keV ($\lambda = 0.0688$ nm), with the incident angle fixed at the critical angle for total external reflection. The incident beam had a size of 0.3×0.3 mm² and a divergence of 0.5 (H) \times 0.1 (V) mrad². The detector slits for GIXD were set for an angular acceptance of 3.5 mrad. A two-dimensional (2D) high grade fiber-optics coupled charge-coupled device detector located at 1.6 m from the sample was used for GISAXS, with 1152×1242 pixels of

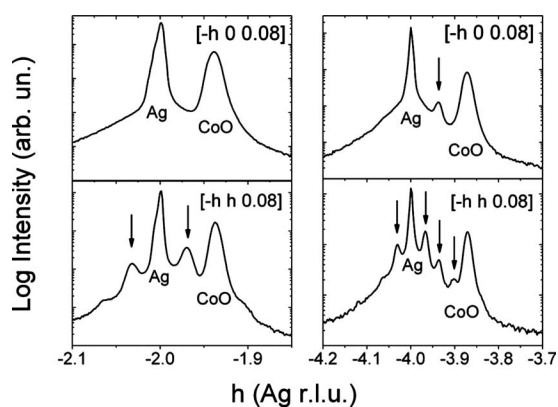


FIG. 1. Radial scans along the $[-h, h, 0.08]$ and $[-h, 0, 0.08]$ directions around the $(-2\ 2\ 0)$ and $(-4\ 4\ 0)$ Bragg peaks of Ag for a 23 ML CoO/Ag(001) sample.

$56.25 \times 56.25\text{ nm}^2$ size. GIXD and GISAXS measurements were performed *in situ*, in UHV, during the growth. In the following, the $(h\ k\ \ell)$ indexed are expressed in reciprocal lattice unit (r.l.u.) of the bulk Ag(001) fcc unit cell (parameter 0.408 nm). (a, b) are the in-plane surface lattice parameters and c is the out-of-plane one.

The substrate used was an Ag(001) single crystal cleaned by repeated cycles of Ar^+ bombardment and annealing at 700 K. CoO(001) films were prepared *in situ* by evaporating Co on the clean Ag surface in 1×10^{-7} mbar of oxygen pressure, at a substrate temperature of 460 K. Ni was next evaporated at room temperature on the CoO(001) surface from a Knudsen cell with a very low evaporation rate of 0.005 nm/min.

The structure of the CoO film deposited on the Ag(001) surface was first investigated by GIXD. Figure 1 shows radial scans around the Ag(220) and (440) Bragg peaks along the $(h, h, 0.08)$ and $(h, 0, 0.08)$ directions for a CoO film of 23 ML of thickness. The epitaxial relationships are the so-called cube-on-cube ones: $\text{CoO}(001)//\text{Ag}(001)$ and $[100]\text{CoO}//[100]\text{Ag}$. Along the $[h, h, 0.08]$ direction, the Bragg peak of CoO is located at $h=1.936$ (Ag r.l.u.) which corresponds to a lattice parameter of 0.2979 ± 0.0005 nm. The value of the CoO parameter, very close to that (0.302 nm¹⁴) of a bulk CoO single crystal, indicates that the strain induced by the mismatch with the Ag substrate is almost completely released at this thickness. Besides the Bragg peaks of Ag and CoO, satellite peaks (marked by arrows in Fig. 1) are found on a periodic network of spacing 0.0325 r.l.u. This observation is in good agreement with the coincidence lattice model (CSL) for coherent interfaces, defined as the smallest lattice in common between the substrate and the overlayer. In a simple picture in which an overlayer grows on a substrate with a different lattice parameter, the result is a 2D distribution of zones of good matching alternating with zones of poor matching. The CSL thus represents the most probable spatial distribution of misfit dislocations. Its period Λ is equal to $a_f/|f|$, a_f being the lattice parameter of the overlayer and $|f|$ the lattice mismatch. For the CoO/Ag(001) interface, $\Lambda=0.2979/0.0325=9.2$ nm.¹⁵ The periodicities of the satellites along the different direction indicate that the

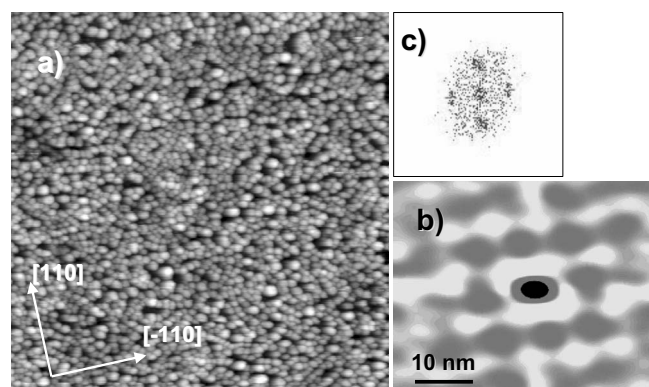


FIG. 2. (a) Constant current topographic STM image of 0.15 nm Ni/20 ML CoO/Ag(001). The image size is $(200 \times 200)\text{ nm}^2$, recorded with $I=0.2$ nA and $V=2.2$ V. (b) 2D self-correlation analysis and (c) Fourier transform of the STM image (a).

dislocations form a squared network with lines running along $\langle 110 \rangle$ directions.^{10,16}

The influence of this dislocation network in the CoO(001) film on the successive growth of a nickel overlayer has been investigated by GISAXS and STM. In Fig. 2, a typical STM image of a thin (0.15 nm) deposit of Ni on 20 ML of CoO(001)/Ag(001) is presented. The surface shows large flat areas uniformly covered by small round Ni clusters. A grain analysis of the STM image shows that the Ni clusters have an average lateral dimension of 4.8 nm and that more than 50% of the clusters have a mean diameter included between 3.8 and 5.8 nm. The height of the clusters varies from 0.3 to 1.3 nm, with an average of 0.6 nm. The initial 3D Volmer-Weber growth of Ni on the CoO surface is not surprising since for thermodynamical reasons 3D is a common growth mode for transition metals on oxides.¹⁷ In addition in the present case there is also a large lattice mismatch between Ni and CoO (21%). The lattice mismatch prevents the epitaxial growth of Ni: the LEED pattern fades increasing the Ni thickness and completely disappears after the deposition of few Ni ML's. We can thus reasonably assume that the Ni overlayer is formed by small crystallites with no preferential orientation.

The self-correlation and Fourier transform analysis of the STM image [Figs. 2(b) and 2(c)] reveal a clear spatial correlation between clusters: they form a square lattice with the sides parallel to the $\langle 110 \rangle$ directions and with a lattice parameter of ~ 8.9 nm. The spatial distribution of the Ni cluster is thus almost identical to the dislocations arrangement.

In situ GISAXS¹⁸ reveals the organization of the Ni clusters, and allows in addition determining the relationships between the locations of the interfacial dislocations and the Ni cluster nucleation centers.¹³ Figure 3(a) shows a GISAXS intensity map measured with the incident x-ray beam parallel to the $\langle 110 \rangle$ crystalline axis before the Ni deposit. Two scattering rods, marked in the figure by black arrows, indicate the presence of a regularly spaced dislocation network in the CoO film.¹⁰ The distance between the two scattering rods and the specular rod is inversely proportional to the separation between the dislocations, yielding again 9.2 nm. Figure

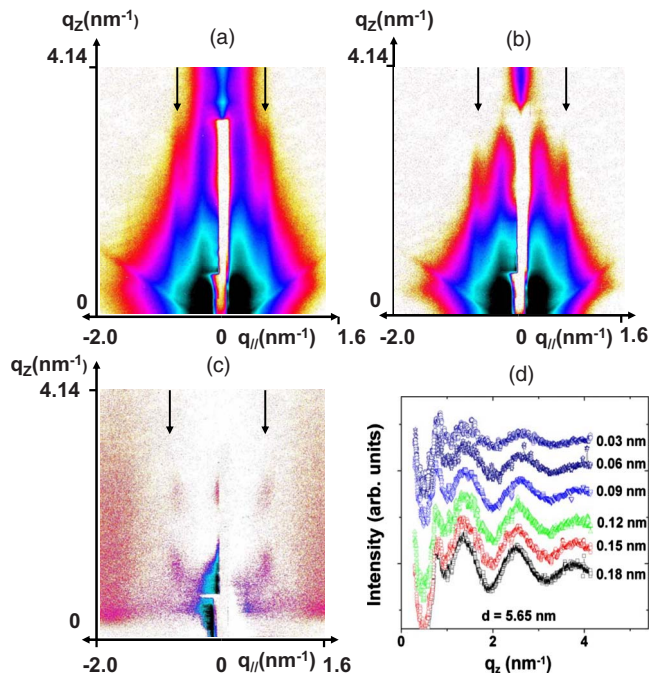


FIG. 3. (Color online) (a) GISAXS image of 25 ML CoO/Ag(001) recorded with the incident beam parallel to the [110] direction. (b) Same image of panel (a) after the deposition of 0.18 nm of Ni. (c) Difference between panel (a) and (b). (d) Sections of panel (c) along the black arrows for different Ni coverages.

3(b) shows the same GISAXS image after the deposition of 0.18 nm of Ni, and Fig. 3(c) shows the difference between the two above images. The intensity of the two scattering rods in the perpendicular direction clearly shows periodic oscillations. This effect arises from the interference between the waves scattered by the dislocation network and the Ni overlayer with increasing perpendicular momentum transfer.¹⁰ The existence of this interference demonstrates that there is a constant separation between the core of the dislocations and the positions of the Ni clusters, and thus that the clusters ordering is induced by the dislocation network. Moreover, the period of the sinusoidal variation as a function of the out of plane momentum transfer [Fig. 3(d)] is in-

versely proportional to the out of plane separation between the dislocation cores (located at the interface), and the Ni clusters. A value of 5.6 nm is obtained, which is in fair agreement with the 25 ML thickness of the CoO film (also checked by out-of plane GIXD measurements). These measurements thus demonstrate that the ordering of the Ni clusters is driven by the presence of the buried dislocation network at the CoO/Ag(001) interface. These findings are of a great relevance because the formation of interfacial dislocations is a common strain relief mechanism in oxide/metal interfaces;^{19–21} it could thus become a useful route to realize the organized growth of metallic nanoparticles on oxide thin films.

In conclusion we have shown that the square interfacial misfit dislocation network formed at the interface between a CoO film and an Ag(001) surface induces a periodic displacement field on the CoO(001) surface, which provides a network of sites for preferential nucleation and growth of metallic nanoparticles. This self-organized growth is achieved at room temperature instead of the more common low temperatures, which shows that the dislocation-induced nucleation sites are strongly energetically favorable. This however necessitates a very low deposition rate for which the diffusion length of the Ni atoms on the oxide surface is of the order of the nanostructuring period. The resulting ordered Ni nanoparticles have a quite narrow size distribution, which is essential to keep well-defined properties over an assembly of nanoparticles. The achievement of the control of the self-assembling process of metal cluster on the surface of a fairly thick (5 nm) oxide film represents a step forward in the production of real devices by self-organized growth. The ~ 10 nm network period corresponds to the ultimate period for possible applications in spintronic or catalysis. Moreover this experiment shows the great potentiality of the GISAXS technique in the study of the self-assembled structures being able to probe, in a nondestructive way, the surface and the buried part of a thin film.

This work is supported by E.U. within the project FP6STRP “GSOMEN” under Contract No. NMP4-CT-2004-001594. E.A.S. also acknowledges financial support from CNPq and FAPEMIG.

¹J. T. Lau, A. Föhlisch, R. Nietubyc, M. Reif, and W. Wurth, *Phys. Rev. Lett.* **89**, 057201 (2002).

²M. Valden, X. Lai, and D. W. Goodman, *Science* **281**, 1647 (1998).

³D. D. Chambliss, R. J. Wilson, and S. Chiang, *Phys. Rev. Lett.* **66**, 1721 (1991).

⁴P. Gambardella, M. Blanc, H. Brune, K. Kuhnke, and K. Kern, *Phys. Rev. B* **61**, 2254 (2000).

⁵B. Voigtländer, G. Meyer, and Nabil M. Amer, *Phys. Rev. B* **44**, 10354 (1991).

⁶A. Ohtake and N. Koguchi, *Appl. Phys. Lett.* **89**, 083108 (2006).

⁷H. Brune, M. Giovannini, K. Bromann, and K. Kern, *Nature*

(London) **394**, 451 (1998).

⁸A. Bourret, *Surf. Sci.* **432**, 37 (1999).

⁹F. Ernult, S. Mitani, K. Takanashi, Y. K. Takahashi, K. Hono, Y. Takahashi, and E. Matsubara, *Appl. Phys. Lett.* **87**, 033115 (2005).

¹⁰F. Leroy, G. Renaud, A. Letoublon, R. Lazzari, C. Mottet, and J. Goniakowski, *Phys. Rev. Lett.* **95**, 185501 (2005).

¹¹G. Cappellini, M. de Seta, C. Spinella, and F. Evangelisti, *Appl. Phys. Lett.* **82**, 1772 (2003).

¹²R. Baudoing-Savois, G. Renaud, M. De Santis, A. Barbier, O. Robach, P. Taunier, P. Jeantet, O. Ulrich, J. P. Roux, M. C. Saint-Lager, A. Barski, O. Geaymond, G. Bérard, P. Dolle, M.

- Noblet, and A. Mougin, Nucl. Instrum. Methods Phys. Res. B **159**, 120 (1999).
- ¹³G. Renaud, R. Lazzari, C. Revenant, A. Barbier, M. Noblet, O. Ulrich, F. Leroy, J. Jupille, Y. Borensztein, C. R. Henry, J. P. Deville, F. Scheurer, J. Mane-Mane, and O. Fruchart, Science **300**, 1416 (2003).
- ¹⁴A. F. Wells, *Structural Inorganic Chemistry* (Clarendon, Oxford, 1984).
- ¹⁵P. Torelli, E. A. Soares, G. Renaud, S. Valeri, X. X. Guo, and P. Luches, Surf. Sci. **601**, 2651 (2007).
- ¹⁶G. Renaud, P. Guenard, and A. Barbier, Phys. Rev. B **58**, 7310 (1998).
- ¹⁷C. T. Campbell, Surf. Sci. Rep. **27**, 111 (1997).
- ¹⁸J. R. Levine, J. B. Cohen, Y. W. Chung, and P. Georgopoulos, J. Appl. Crystallogr. **22**, 528 (1989).
- ¹⁹J. Wollschlager, D. Erdos, H. Goldbach, R. Hopken, and K. M. Schroder, Thin Solid Films **400**, 1 (2001).
- ²⁰M. Dynna, J. L. Vassent, A. Marty, and B. Gilles, J. Appl. Phys. **80**, 2650 (1996).
- ²¹S. Benedetti, H. M. Benia, N. Nilius, S. Valeri, and H. J. Freund, Chem. Phys. Lett. **430**, 330 (2006).